Interactive effect of age and *APOE-ε4* allele load on white matter myelin content in cognitively normal middle-aged subjects

Grégory Operto[a], José Luis Molinuevo[a,b,c], Raffaele Cacciaglia[a], Carles Falcon[a,d],
Anna Brugulat-Serrat[a], Marc Suárez-Calvet[a], Oriol Grau-Rivera[a], Nuria Bargalló[b,e],
Sebastián Morán[f], Manel Esteller[f,g,h], for the ALFA Study[1], Juan Domingo Gispert[a,c,*]

[a] *Barcelonaβeta Brain Research Center, Pasqual Maragall Foundation, Barcelona, Spain*
[b] *Institut d'Investigacions Biomèdiques August Pi i Sunyer (IDIBAPS), Barcelona, Spain*
[c] *CIBER Fragilidad y Envejecimiento Saludable (CIBERFES), Madrid, Spain*
[d] *Centro de Investigación Biomédica en Red de Bioingeniería, Biomateriales y Nanomedicina (CIBER-BBN), Madrid, Spain*
[e] *Centre Mèdic Diagnòstic Alomar, Barcelona, Spain*
[f] *Cancer Epigenetics and Biology Program (PEBC), Bellvitge Biomedical Research Institute (IDIBELL), L'Hospitalet, Barcelona, Spain*
[g] *Departament de Ciències Fisiològiques II, Escola de Medicina, Universitat de Barcelona, Barcelona, Spain*
[h] *Institució Catalana de Recerca i Estudis Avançats (ICREA), Barcelona, Spain*

ARTICLE INFO

ABSTRACT

The apolipoprotein E gene (*APOE*) ε4 allele has a strong and manifold impact on cognition and neuroimaging phenotypes in cognitively normal subjects, including alterations in the white matter (WM) microstructure. Such alterations have often been regarded as a reflection of potential thinning of the myelin sheath along axons, rather than pure axonal degeneration. Considering the main role of *APOE* in brain lipid transport, characterizing the impact of *APOE* on the myelin coating is therefore of crucial interest, especially in healthy *APOE-ε4* homozygous individuals, who are exposed to a twelve-fold higher risk of developing Alzheimer's disease (AD), compared to the rest of the population.

We examined T1w/T2w ratio maps in 515 cognitively healthy middle-aged participants from the ALFA study (ALzheimer and FAmilies) cohort, a single-site population-based study enriched for AD risk (68 *APOE-ε4* homozygotes, 197 heterozygotes, and 250 non-carriers). Using tract-based spatial statistics, we assessed the impact of age and *APOE* genotype on this ratio taken as an indirect descriptor of myelin content.

Healthy *APOE-ε4* carriers display decreased T1w/T2w ratios in extensive regions in a dose-dependent manner. These differences were found to interact with age, suggesting faster changes in individuals with more ε4 alleles.

These results obtained with T1w/T2w ratios, confirm the increased vulnerability of WM tracts in *APOE-ε4* healthy carriers. Early alterations of myelin content could be the result of the impaired function of the ε4 isoform of the *APOE* protein in cholesterol transport. These findings help to clarify the possible interactions between the *APOE*-dependent non-pathological burden and age-related changes potentially at the source of the AD pathological cascade.

1. Introduction

The ε4 allele of the apolipoprotein E gene (*APOE*), which is the main genetic risk factor for late-onset Alzheimer's disease (AD), has also a strong and manifold impact neuroimaging phenotypes (Reinvang et al., 2013; Fouquet et al., 2014) in cognitively normal subjects. In

cognitively intact individuals, carrying the ε4 allele has been shown to exert a dose-dependent influence on amyloid accumulation (Reiman et al., 2009), glucose metabolism (Reiman et al., 2001) and the brain structure at macro- and microscopic levels (Fouquet et al., 2014). Effects of *APOE*-ε4 on gray matter have been assessed by many studies (Cacciaglia et al., 2018; Protas et al., 2013; Lemaitre et al., 2005; Chen et al., 2007). A growing body of evidence has also been supporting an association between the *APOE*-ε4 status and white matter (WM) integrity. A review of existing results was included in Operto et al., 2018. In this recent study, microstructural alterations in WM integrity have been reported in cognitively normal carriers of the ε4 allele using diffusion-weighted imaging (DWI), with the largest differences involving higher mean (MD) and radial (RD) rather than changes in axial diffusivity (AxD), in extended regions including bilateral main associative tracts. Such directional pattern in diffusion metrics has often been regarded as a reflection of potential thinning of the myelin sheath, rather than Wallerian degeneration (Wang et al., 2015; Zhang et al., 2012; Song et al., 2002). Myelin quantification requires the implementation of specific imaging protocols (see Heath et al. (2018) for a recent review). Otherwise, myelination cannot be strictly measured using standard single-shell DWI techniques and can only be speculated through the appreciation of combined diffusivity metrics.

Myelin is produced by oligodendrocytes in the central nervous system and forms an insulating layer around axons, which provides key core functions related to signal transmission. Given the main role of *APOE* in the transport of cholesterol which is a major component of myelin, the observed lower functionality of the ε4 isoform is suspected to contribute to the increased risk to AD observed in ε4-carriers (Liu et al., 2013a).

Impacts of common risk factors on demyelination and its contribution to cognitive decline are suspected but have been poorly investigated in human populations (Dean et al., 2015; Peters, 2002). Bartzokis and colleagues have introduced a model describing the course of myelin integrity across lifespan, following an inverted U-shape (Bartzokis, 2011), its association with cognitive efficiency metrics (Lu et al., 2013) and how its breakdown may relate to neuropathological processes such as incipient AD (Bartzokis, 2004; Bartzokis et al., 2007). Some results have also supported the proposed concept of *retrogenesis,* suggesting that the latest tracts to myelinate would be the most vulnerable to age and pathologies, and therefore the first to disrupt (Benitez et al., 2014; Gao et al., 2011; Stricker et al., 2009; Brickman et al., 2012; Reisberg et al., 2002). AD-related myelin changes have long been considered as secondary aging effects and hence literature on the subject is still lacking. Dean et al. (2017) in a recent study report widespread age-related changes especially in late-myelinating brain regions and negative associations between relaxometry measures across WM and levels of CSF biomarkers in cognitively asymptomatic participants. Bouhrara et al. (2018) showed decreased myelin water fraction in subjects suffering mild cognitive impairment, vascular dementia or AD, compared with old controls. Altogether these results shed light on the role myelin and oligodendrocytes may play in the AD continuum and support a potentially emerging value of myelination as biomarker, in line with the recent attention given to micro- and macrostructural changes in WM in the risk and progression of AD (Nasrabady et al., 2018).

It has been proposed that the ratio of T1-weighted (T1w) over T2-weighted (T2w) Magnetic Resonance Imaging (MRI) intensities could render myelin-enhanced contrast images (Glasser et al., 2014), which may be well-suited in contexts where specific multi-compartment acquisitions are not available or feasible. The method is based on the assumption that histological measures of myelin content covary with both T1w and T2w intensity, but in opposite directions (Glasser and Van Essen, 2011). It was initially proposed for cortical mapping of myelin, then was extended to the whole brain (Ganzetti et al., 2014) and met a variety of applications with special emphasis in developmental studies (Lee et al., 2015; Soun et al., 2017; Lebel and Deoni,

2018), neurodegenerative diseases e.g. MS (Righart et al., 2017), schizophrenia (Iwatani et al., 2015), Alzheimer's disease (Yasuno et al., 2017; Pelkmans et al., 2019) and the healthy brain (Shafee et al., 2015).

The present study aims at studying the impact of *APOE*-ε4 allele load on white matter myelin, using T1w/T2w maps as a proxy for myelin content, and its interaction with age. To this end, we generated T1w/T2w ratio maps following the approach introduced by Glasser and Van Essen (2011) and performed group analysis using non-parametric skeleton-based statistics focused on WM tracts (Smith et al., 2006). Such method has been extensively used to explore microstructural changes using diffusion metrics and still to our knowledge has never been employed before for this type of data.

Our initial hypothesis was based on that if previous differences observed with DWI were due to changes in white matter myelination, then those changes would potentially be captured by T1w/T2w maps. We hence hypothesized that subjects at risk of developing AD would show negatively affected ratio values in regions matching the differences observed in diffusion imaging (long associative tracts) (Operto et al., 2018). The high number of *APOE*-ε4 homozygotes allowed us to better understand the impact of this allele according to the number of carried copies on the microstructural properties of the brain. We assessed the effects of *APOE*-ε4 load, status, age, and sex. We hypothesized that T1w/T2w ratio values would decline with age, as expected with the course of myelination at this age range. Effect of sex was reported for exploratory purposes. Age by genotype interaction was also tested.

2. Methods and materials

2.1. Study participants

The participants of this study were recruited in two steps. In a first phase, 2743 cognitively healthy volunteers aged between 45 and 74 years were registered in the ALFA study (ALzheimer and FAmilies), a large cohort program aimed at identifying neuroimaging biomarkers of preclinical AD in the general population (Molinuevo et al., 2016). Exclusion criteria included performance below established cutoffs for a number of cognitive tests as well as the presence of any psychiatric or any other clinically significant condition (Molinuevo et al., 2016). In a second phase, after *APOE* genotyping, cerebral MRI examination was proposed to all participants homozygous (HO) for the ε4 allele and all carriers of the ε2 allele, along with ε4-heterozygous (HT) and non-carriers (NC) matched for age and sex. This strategy resulted in the selection of 576 study participants, 61 of whom had to be excluded because of either MRI incidental findings (32), poor image quality (12) or processing issue (17), resulting in a final sample size of 515. Demographic characteristics of the participants are summarized in Table 1.

For the statistical analyses, participants were pooled according to the cumulative number of ε4 alleles, that is, noncarriers as well as ε4-heterozygous and ε4-homozygous individuals. Since homozygous subjects were significantly younger than noncarriers and heterozygotes (Table 1), age was included as a covariate in all subsequent analyses.

2.2. APOE genotyping

Total DNA was obtained from the blood cellular fraction by proteinase K digestion followed by alcohol precipitation. Samples were genotyped for two single nucleotide polymorphisms (SNPs), rs429358 and rs7412, determining the possible *APOE* isoforms: ε1, rs429358 (C) + rs7412 (T); ε2, rs429358 (T) + rs7412 (T); ε3, rs429358 (T) + rs7412 (C); and ε4, rs429358 (C) + rs7412 (C). Of the 515 participants, 153 were ε3/ε4 carriers, 146 were homozygous for the ε3 allele, 104 were ε2/ε3 carriers, 68 were homozygous for the ε4 allele and 44 were ε2/ε4. The allele frequencies were in Hardy-Weinberg equilibrium.

Table 1
Sample characteristics.

	Total sample (N = 515)		NC (N = 250)		HT (N = 197)		HO (N = 68)		Inferential statistics
	M	SD	M	SD	M	SD	M	SD	
Age[a]	58.00	7.41	58.40	7.55	58.57	7.35	54.94	6.18	F = 6.88; $p < .01$
Education[a]	13.64	3.57	13.62	3.61	13.75	3.53	13.38	3.46	F = 0.27; $p = .76$
MMSE[b]	29.04	1.08	29.00	1.12	29.02	1.10	29.26	0.77	F = 1.54; $p = .22$
TFR[b]	16.47	5.16	16.23	5.15	16.37	5.12	17.73	5.12	F = 2.24; $p = .11$
TPR[b]	24.11	4.50	23.72	4.84	24.24	4.23	25.19	3.68	F = 2.84; $p = .06$
WMH[c]	3.18 [1.09, 3.65]		3.22 [1.13, 3.41]		3.03 [1.08, 3.70]		3.47 [1.13, 3.82]		H = 0.60; $p = .65$
Fazekas scales	**0:** 247 **1:** 221 **2:** 39 **3:**2		**0:** 113 **1:** 115 **2:** 17 **3:** 2		**0:** 101 **1:** 80 **2:** 14		**0:** 33 **1:** 26 **2:** 8		$\chi^2 = 3.82$; $p = .43$
Male/female	201/314		88/162		88/109		25/43		$\chi^2 = 4.32$; $p = .12$

NC = APOE-ε4 Non-carriers; HT = APOE-ε4 Heterozygous; HO = APOE-ε4 Homozygous; MMSE = Mini-Mental State Examination score; TPR = Total Paired Recall; TFR = Total Free Recall;; WMH = White Matter Hyperintensities; M = mean; SD = standard deviation.

[a] Indicated in years.
[b] Cognition data was not available for 15 subjects.
[c] Indicated in mL. Mean value is presented along with first and third quartiles. Data was not available for 6 subjects.

2.3. Cognitive measures

The Memory Binding Test (MBT) (Buschke, 2014) was used to evaluate verbal episodic memory. This test assesses immediate and delayed retention of verbal information (after a lapse of 25 to 35 min) through a controlled learning process of two lists of 16 words belonging to 16 different semantic categories presented in the same order. Further detail on the administration procedure of the MBT and an exhaustive description of each of the variables can be found in (Gramunt et al., 2015). MBT yielded seven main outcomes corresponding to two main areas: learning and immediate recall, and delayed recall. Executive function was assessed by means of five WAIS-IV subtests: the Digit span (immediate and working memory): forward, backward and sequencing; Coding subtest (processing speed and attention); Matrix reasoning and Visual puzzles (fluid intelligence); and Similarities (abstract verbal reasoning). We summarized these scores in two Z scores, one for memory and one for executive functions, by computing arithmetic means of individual Z scores from the original score values.

2.4. Image data acquisition

All brain MRI data were acquired on a single standard 3 T General Electric scanner (GE Discovery MR750 W). Structural 3D high-resolution T1-weighted images were collected in the sagittal plane using a fast spoiled gradient-echo (FSPGR) sequence implementing the following parameters: voxel size = 1 mm³ isotropic, Repetition Time [TR] = 6.16 ms, Echo Time [TE] = 2.33 ms, Inversion Time [TI] = 450 ms, matrix size = 256 × 256 × 174, flip angle = 12°. T2 and T2*-weighted sequences were acquired in the axial plane with a voxel size of 1 × 1 × 3 mm and the following parameters: fluid attenuation inversion recovery (FLAIR: TR/TE/TI = 11,000/90/2600 ms, flip angle = 160°), fast spin echo (TR/TE = 5000/85 ms, flip angle = 110°), and gradient echo (GRE: TR/TE = 1300/23 ms, flip angle = 15°).

The DWI protocol employed a spin-echo echo-planar imaging sequence with one T2-weighted baseline (b = 0), 64 b = 1000 s·mm⁻² diffusion-weighted volumes acquired with 64 distinct diffusion-encoding directions. The field of view was 256 × 256 mm, and the imaging matrix was 128 × 128 with 56 slices and slice thickness 2 mm, giving 2-mm isotropic voxels.

All scans were visually assessed for quality and incidental findings by a trained neuroradiologist (Brugulat-Serrat et al., 2017). This resulted in the exclusion of ten participants due to the presence of a meningioma, and of 37 participants due to susceptibility, motion artifacts or segmentation problems, resulting in a total of 515 images ready for subsequent analyses.

2.5. Image processing

The general workflow included first the generation of individual T1w/T2w maps, then the group analysis over the main fiber tracts of WM.

2.5.1. Generation of individual T1w/T2w ratio maps

T1w and T2w images were converted to NIfTI format and analyzed using a similar method as proposed by Glasser and Van Essen (2011). Brain mask extraction was performed on raw T1w images using FSL BET to facilitate subsequent coregistration with T2w images. BET's parameters were fine-tuned for every subject so as to achieve correct brain extraction after individual visual inspection. Raw T2w images were then rigidly coregistered over T1 masked images using the ANTs toolbox (using mutual information as cost function) (Avants et al., 2009) and ratio maps were generated dividing T1 by T2 intensities. Since group analysis is done over a skeletonized version of WM obtained using DWI data, T1w/T2w ratio maps were aligned to DWI b = 0 maps using ANTs elastic coregistration.

2.5.2. Creation of the WM skeleton and projection of the data

DWI images were first denoised with the overcomplete local PCA method by Manjón et al. (2013), then corrected for eddy current distortions and head motion (using FSL's eddy_correct, default parameters). Data analysis was then performed using tools from the FMRIB Software Library software suite (Jenkinson et al., 2012). Fractional anisotropy (FA), MD, AxD and RD maps were generated using DTIFit that fits a diffusion tensor model at each voxel. The FA output images were used as input for Tract-Based Spatial Statistics (TBSS) (Smith et al., 2006). TBSS is a pipeline - part of the FSL toolbox - which has been broadly used in DWI studies, including an image processing and statistical analysis part, both carried out consecutively. In this pipeline, intersubject matching is achieved by projecting unsmoothed data on skeletons representing the center of the WM fiber bundles and subsequent statistical analysis is done on the projected data relying on a non-parametric permutation-based technique, hence mitigating some limitations of the standard voxel-based morphometric approach. It consists of the following steps. All subjects' FA data were coregistered to the FMRIB58 FA template using FMRIB's Non-linear Image Registration Tool (FNIRT). The mean FA image was generated and then "thinned", by non-maximum-suppression perpendicular to the local tract structure, to create a mean FA skeleton, which represents the centers of all tracts common to the group. The mean skeleton was thresholded and binarized at FA > 0.2. T1w/T2w maps were warped to the same intersubject reference space using individual transformations obtained from the coregistration of the FA maps. Each subject's aligned data - including FA and T1w/T2w maps - was finally projected onto the mean
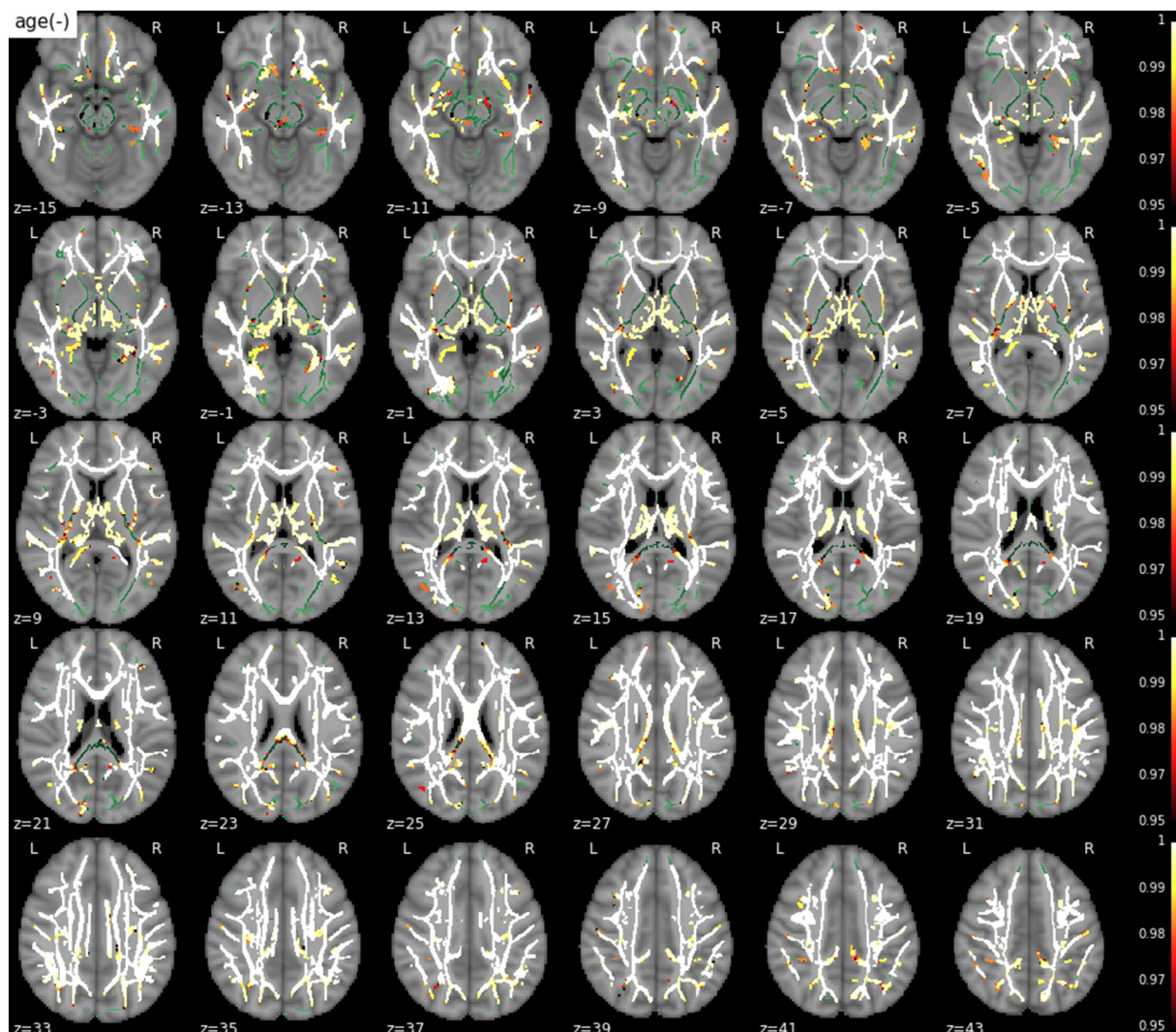
Fig. 1. Main effect of age on T1w/T2w ratio. A strong negative association was found between age and T1w/T2w ratio in extensive regions. The WM skeleton is shown in green. Supra-threshold clusters are presented in colors from dark red to white (1-p > .95, familywise error rate- and threshold-free cluster enhancement-corrected).

FA skeleton and the resulting projected data fed into voxelwise group analysis.

2.6. Statistical analysis

Group-related differences were assessed using a voxel by voxel permutation nonparametric test (5000 permutations) with threshold-free cluster enhancement, as performed by the Randomise tool available in FSL (Winkler et al., 2014). All results are shown at $P < .05$ corrected for multiple comparisons across space. Correction for multiple testing was applied using the default familywise error rate control with threshold-free cluster enhancement as implemented in Randomise and as described elsewhere (Winkler et al., 2014; Smith and Nichols, 2009).

We performed voxelwise multiple linear regression analysis using two main models, the first one to measure the effect of the number of APOE-ε4 alleles on skeletonized T1w/T2w maps and the second one which modeled the interaction effect with age on top of the main effect of APOE genotype. We partitioned genetic variance by including three dummy regressors coding for the number of ε4 alleles carried. The first model included age and sex as confounding variables (5 regressors in total). The second one only included sex, as age by genotype interaction was the effect of interest. Considering the expected nature of the course

of myelination across time, age was modeled as a quadratic term centered at age 50, matching with descriptions from lifespan studies (Sherin and George, 2011; Yeatman et al., 2012; Grydeland et al., 2018). This second model resulted in a design matrix with 7 regressors, one for sex as covariate, 3 for the dummy-coded APOE genotypic groups (NC, HT, HO; main effect) and 3 for the interaction between APOE and age^2 (centered at 50 years).

We compared T1w/T2w ratios to assess the different components of the effects of APOE genotype among dominance (ε4 carriers versus non-carriers), recessivity (homozygotes versus others) and additivity (correlation with the number of ε4 alleles carried), in both directions (positive and negative correlations).

2.7. Supplementary analyses

In order to control for potential biasing effects in our dataset and to compare results across modalities, we repeated the analysis using the exact same models/contrasts over parametric maps obtained by DWI on the same participants. The first model (main effect of APOE) matches the one used in Operto et al., 2018. The second one (interaction with age) is the same as the one used with T1w/T2w ratio maps. Results are presented in Appendix A (Supplementary Data).

A complementary analysis was performed to rule out the potential
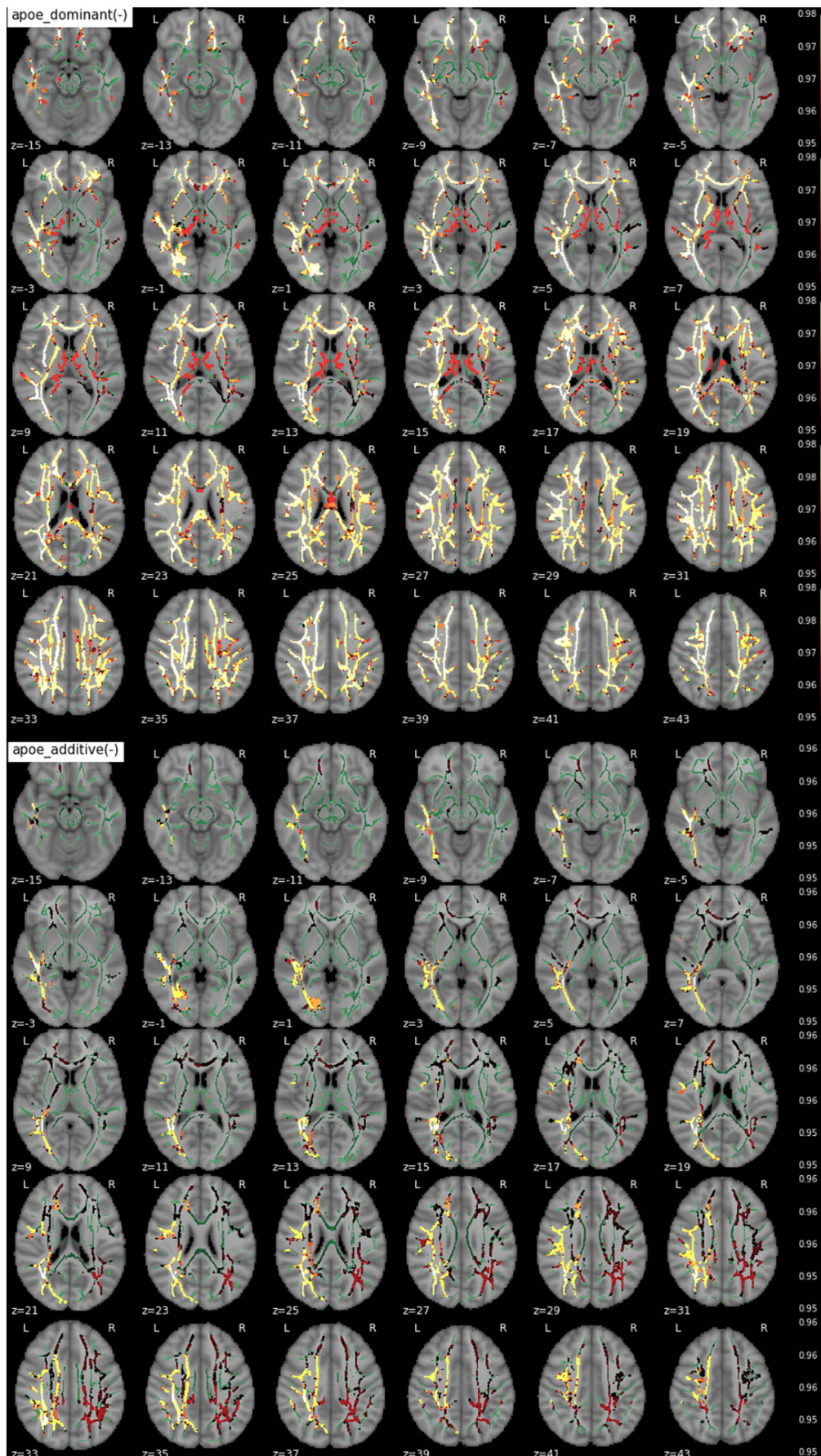
(caption on next page)

Fig. 2. - Effect of the number of *APOE-ε4 alleles* on T1w/T2w (from top to bottom - dominant and additive components) -.
no recessive component was observed - only contrast maps associated with lower T1w/T2w in ε4 carriers showed significant voxels. The WM skeleton is shown in green. Supra-threshold clusters are presented in colors from dark red to white (1-p > .95, familywise error rate- and threshold-free cluster enhancement-corrected).
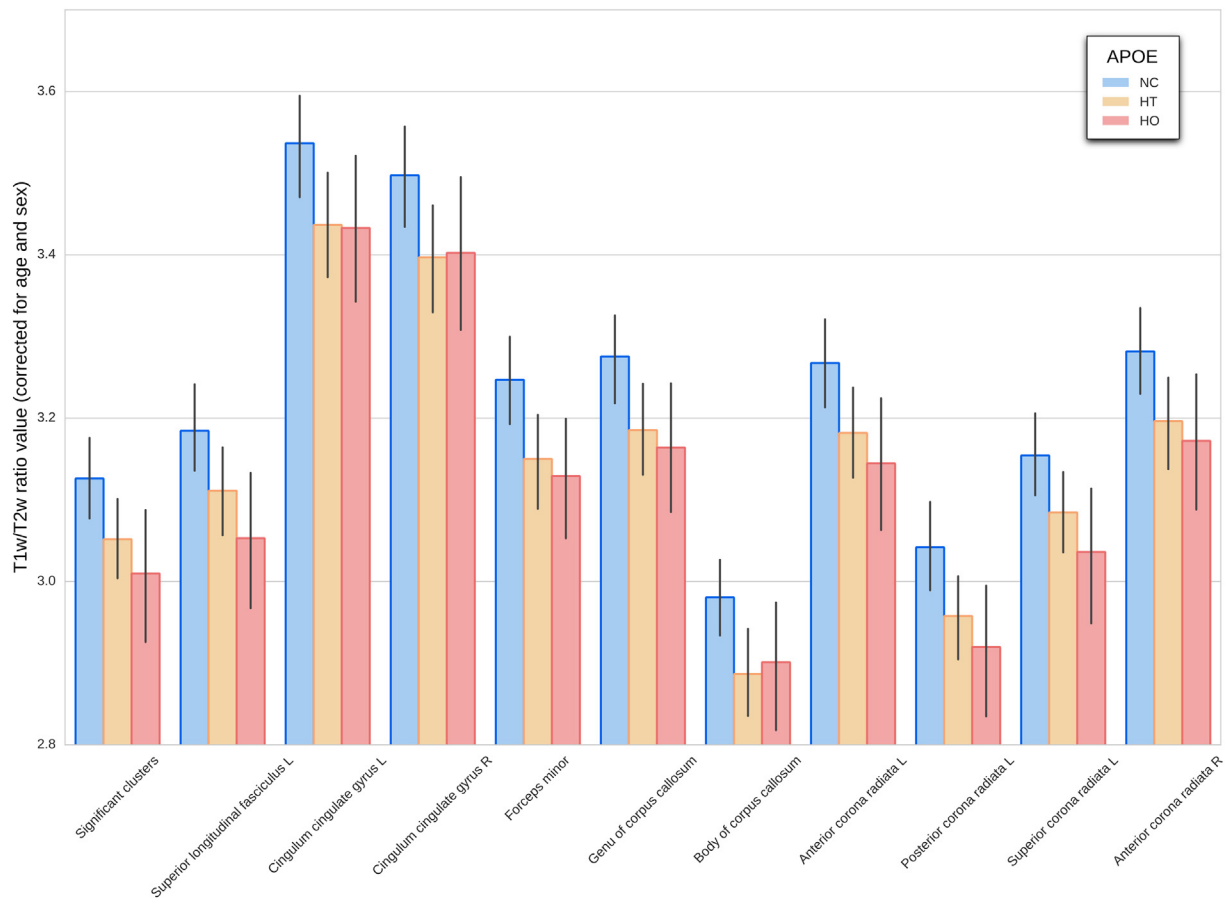
Fig. 3. Main effect of the number of *APOE-ε4* alleles on T1w/T2w ratio across fiber tracts. Each bar represents the mean value extracted from the corresponding tract ROI (from the Johns Hopkins University white matter atlas) along with standard error (confidence interval: 95%). Significant tracts are displayed only ($p < .05$ familywise error rate corrected). NC = *APOE-ε4* Non-carriers; HT = *APOE-ε4* Heterozygous; HO = *APOE-ε4* Homozygous.

impact of white matter hyperintensities (WMH), both at global and voxel-wise levels. To this end, WMH masks were segmented from fluid-attenuated inversion recovery images of the same individuals using a method described previously (Sudre et al., 2015; Operto et al., 2018) and any voxel identified as a lesion in any subject of the studied sample was removed from the analysis. A threshold of 0.9 was used on the original probability maps yielded by the segmentation algorithm to generate binary masks which were fed into TBSS to exclude lesion voxels from the analysis. Global effects of WMH load were also assessed by introducing global WMH volumes as confounders in the statistical models. Independently, potential impact of pathological levels of WMH was evaluated by using Fazekas scores instead as confounders.

We also looked for potential associations between T1w/T2w ratio values and cognitive scores assessed by memory and executive tasks. We used different models for each score among total paired recall (TPR), total free recall (TFR), coding subtest (processing speed) and the two Z scores measuring memory and executive functions, respectively, including - for each of these models - age, sex and *APOE* genotype as confounders.

3. Results

3.1. Main effect of age

There was a significant main effect of age on T1w/T2w ratio in the vast majority of the skeletonized WM (Fig. 1), demonstrating previously well-documented results regarding age-related changes in myelination through late-middle age.

3.2. Main effect of APOE genotype

We found significant main effects of *APOE-ε*4 on the T1w/T2w maps. Fig. 2 shows the TBSS map for the significant clusters where *APOE-ε*4 carriers displayed decreased values compared with non-carriers in extended regions of the skeletonized WM. These regions included forceps minor, bilateral superior longitudinal fasciculus (SLF), corpus callosum, corona radiata, inferior fronto-occipital fasciculus (IFOF), left inferior longitudinal fasciculus (ILF) and left anterior thalamic radiation (ATR) (tracts from the John Hopkins University Atlas (Wakana et al., 2004)). The observed effects reached statistical significance for the dominant and additive models, therefore suggesting significant differences between non-carriers and carriers and also in a dose-dependent manner. Significant clusters in the additive contrast map share a 48% of suprathreshold voxels with the dominant contrast,
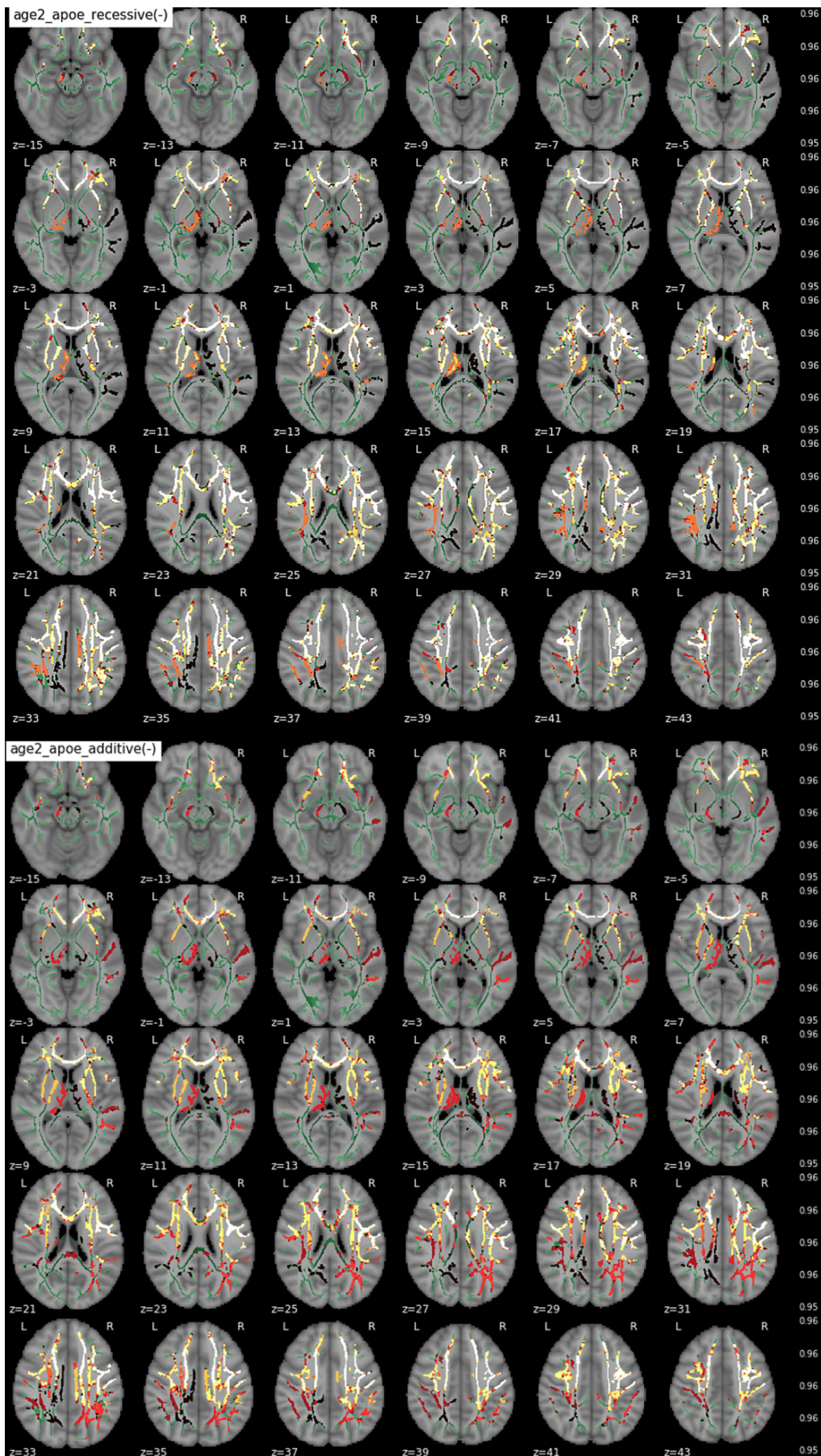
(caption on next page)

Fig. 4. Interaction between age and *APOE-ε*4 on T1w/T2w (from top to bottom - recessive and additive components) -.
no dominant component was observed - only contrast maps associated with lower T1w/T2w in ε4 carriers showed significant voxels. The WM skeleton is shown in green. Supra-threshold clusters are presented in colors from dark red to white (1-p > .95, familywise error rate- and threshold-free cluster enhancement-corrected).

while the vast majority (> 99%) of voxels from the additive contrast were also significant in the dominant one. Fig. 3 represents these changes between *APOE* groups across fiber tracts.

3.3. Interaction APOE genotype x age

We found a significant negative interaction between the number of *APOE-ε*4 alelles and age in extensive bilateral regions of the WM in both the recessive and the additive contrast (Fig. 4). These regions included, by decreasing order of spatial extent, forceps minor, bilateral SLF, ATR, corona radiata, right IFOF and corpus callosum in both contrasts. Significant clusters in the additive contrast map share a 93% of supra-threshold voxels with the recessive contrast. In these areas ε4 carriers displayed significantly decreased T1w/T2w ratio with respect to non-carriers. This effect was shown to be dose-dependent with respect to the number of ε4 alleles and stronger in ε4 homozygotes compared to the rest of the subjects. Fig. 5 plots values derived from bilateral SLF with respect to age and genotype group (corrected for sex), hence depicting how T1w/T2w ratio taken in SLF depart in homozygotes as compared to other groups.

3.4. Main effect of sex

T1w/T2w ratios were significantly lower in male participants in a limited set of regions (Fig. 6), mainly in the left hemisphere, including left SLF, ILF and IFOF and part of the forceps major.

3.5. Association with cognitive performance

We found no significant association between any cognitive score (among TPR, TFR, coding subtest and Z scores for memory/executive functions) and T1w/T2w ratios.

3.6. Effect of vascular factors

No voxel demonstrated a significant association between any parametric map and global volumes of WM lesions or Fazekas scores in this dataset. Similarly, no global or regional effect of WMH load was detected in these respective complementary analyses.

4. Discussion

Myelin alterations in subjects at risk of developing AD are still understudied to date in comparison to existing literature on microstructural integrity as measured using DWI. In contrast, changes in diffusion metrics have regularly been interpreted as potentially indicating a loss in myelin content in subjects at risk of developing the disease. Still, myelin cannot be measured using standard single-shell DWI, and can only be speculated through the appreciation of combined diffusivity metrics. We hypothesized that subjects at risk of developing AD would show negatively affected ratio values in regions matching the ones observed in diffusion imaging taking T1w/T2w ratios as indirect measures of myelin content. T1w/T2w ratio has been extensively used in previous research as a non-quantitative descriptor of cortical myelination, but rarely in WM studies (Chen et al., 2017). Results from this present study show significant decreases of this ratio in *APOE-ε*4 carriers in extended regions of the WM in a cognitively normal population. Across all tested models/contrasts, *APOE-ε*4 carriers never showed significant increases of this ratio. The previously described patterns in DWI (increased RD and MD but not AxD) together with similar results in healthy infants (Dean et al., 2014), support our previous
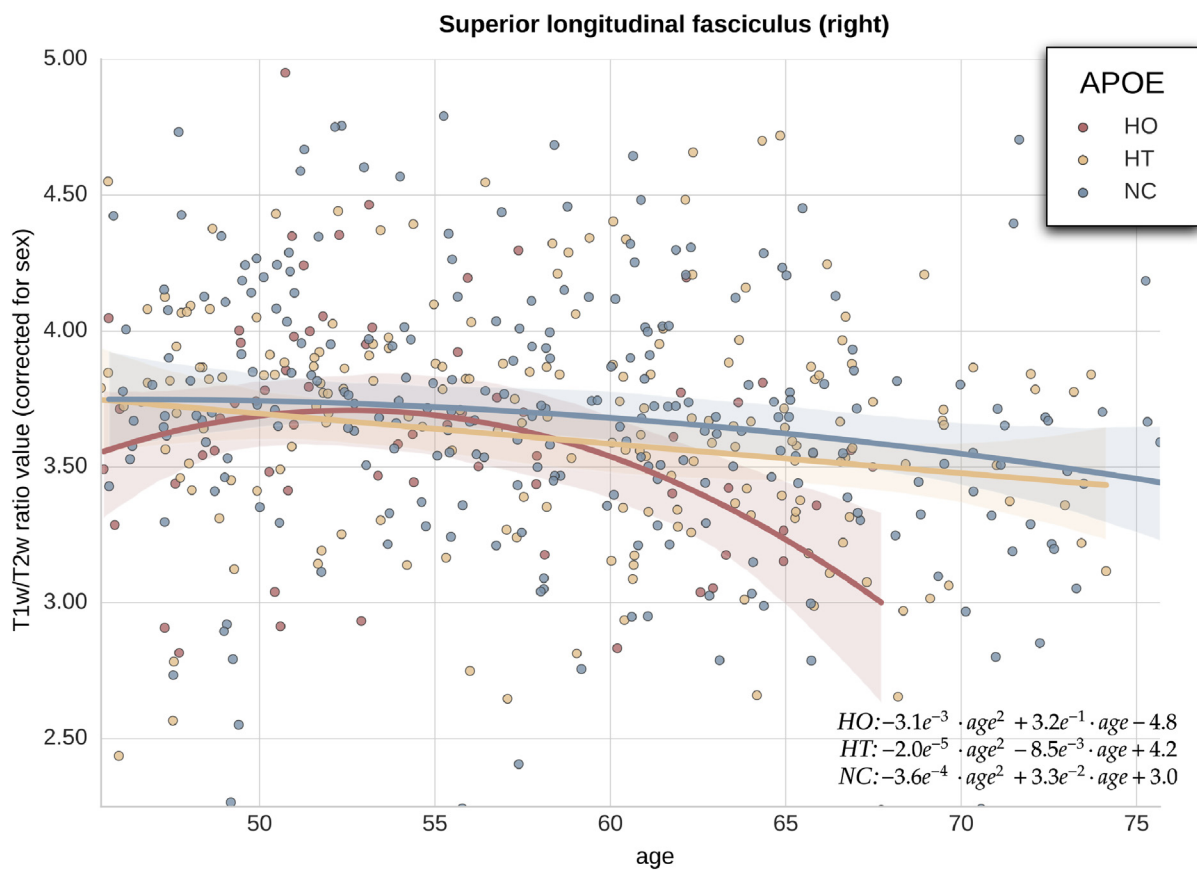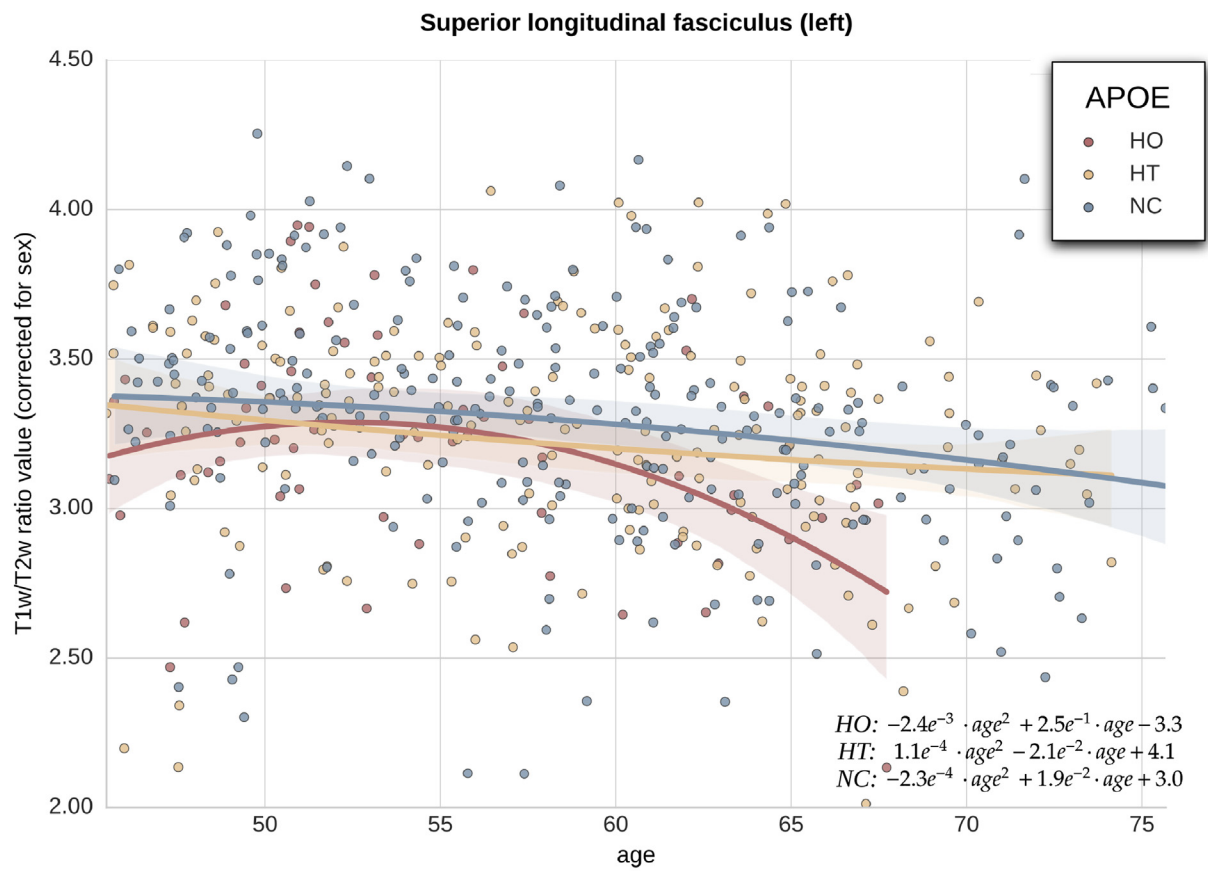
interpretation that such changes would reflect developmental alterations related to myelin content in ε4 cognitively carriers. As speculated in Operto et al. (2018), by lacking functional isoforms of the ApoE protein, ε4 homozygotes may have thinner myelin sheaths than what would correspond to their age. Altered myelination would impact negatively transmission speed and consequently require a higher metabolic consumption to sustain cognitive performance within normality. As a result, and in combination with other metabolic deficits observed in cognitively normal ε4 carriers, these changes might contribute to the increased vulnerability of this group to brain insults associated with AD.

On the other hand, the interaction between *APOE-ε*4 and age observed in the present study can be interpreted as a higher vulnerability of carriers to age-related processes and/or the presence of AD pathological changes. Importantly, differences in T1w/T2w were found significant in both dominant and additive contrasts, suggesting a main effect of the ε4 allele in a dose-dependent manner. Mirroring previous observations made in DWI studies, the effects of *APOE* on this ratio are observed in extensive regions of the white matter. In particular, SLF, known to be primarily affected in AD (Adluru et al., 2014; Douaud et al., 2011; Pievani et al., 2010; Stricker et al., 2009) and in mild cognitive impairment (Liu et al., 2013b; Amlien and Fjell, 2014), was among the tracts showing the strongest association. Some of the largest effects are also found in forceps minor and long associative tracts such as bilateral SLF, ILF, IFOF. Commissural fibers (e.g. corpus callosum and forceps minor) or limbic system tracts (cingulum) tend to show a rather dominant effect. In contrast, associative tracts (SLF, ILF, IFOF) display a more additive one. Associative tracts are also known to be composed of late-myelinating fibers (Welker and Patton, 2012), hence potentially more vulnerable (Benitez et al., 2014) according to the retrogenesis model.

We also replicated previous observations from Operto et al. (2018) using the same model/contrasts on DWI data, still without finding any interaction between age and ε4 status in that modality. Several studies reported different age trajectories of DWI metrics across *APOE* groups in cognitively normal participants, in particular in older samples. In this respect, it might be interpreted that T1w/T2w ratio maps show a higher sensitivity as compared to diffusion imaging to detect myelin-related changes. Still, such difference across modalities is open to various possible interpretations: either the measures provided by the two modalities may address the same common entity, e.g. myelination, therefore such difference would indeed reflect a higher sensitivity of T1w/T2w ratio in detecting the onset of demyelination as compared to DWI; or these measures could possibly relate to compounds which are different albeit related, with T1w/T2w consequently capturing the earlier of two sequential events, while effect on DWI would still be independent of age at that current stage. Head to head comparison and the assessment of the longitudinal evolution of these measurements against more specific measurements of myelin content are required to explore further these dynamics.

T1w/T2w ratio was initially proposed as an indirect, non-quantitative, measure of myelin content (Glasser et al., 2014) and rapidly met interest in a substantial amount of studies (Shafee et al., 2015). A number of considerations have also been raised over the years regarding reliability with respect to tailored acquisition protocols (Deoni et al., 2008; Heath et al., 2018; Hagiwara et al., 2018), or other factors e.g. tissues or groups with different pathological conditions. Some authors also advocate for bias correction and intensity normalization prior to T1w/T2w ratio calculation (Ganzetti et al., 2014) in particular to compensate for interscanner variability in the context of multisite studies. We believe that having acquired it on a single scanner on

Superior longitudinal fasciculus (left)

$$HO: -2.4e^{-3} \cdot age^2 + 2.5e^{-1} \cdot age - 3.3$$
$$HT: \ 1.1e^{-4} \cdot age^2 - 2.1e^{-2} \cdot age + 4.1$$
$$NC: -2.3e^{-4} \cdot age^2 + 1.9e^{-2} \cdot age + 3.0$$

Superior longitudinal fasciculus (right)

$$HO: -3.1e^{-3} \cdot age^2 + 3.2e^{-1} \cdot age - 4.8$$
$$HT: -2.0e^{-5} \cdot age^2 - 8.5e^{-3} \cdot age + 4.2$$
$$NC: -3.6e^{-4} \cdot age^2 + 3.3e^{-2} \cdot age + 3.0$$

Fig. 5. Effect of aging and the number of *APOE-ε4* alelles on T1w/T2w ratios (unitless) in the SLF area. Each dot represents a subject (red: ε4 homozygotes [HO], orange: ε4 heterozygotes [HT], blue: non-carriers [NC]). Quadratic regression (by age correcting for sex) is displayed (solid curves) for each *APOE* group.
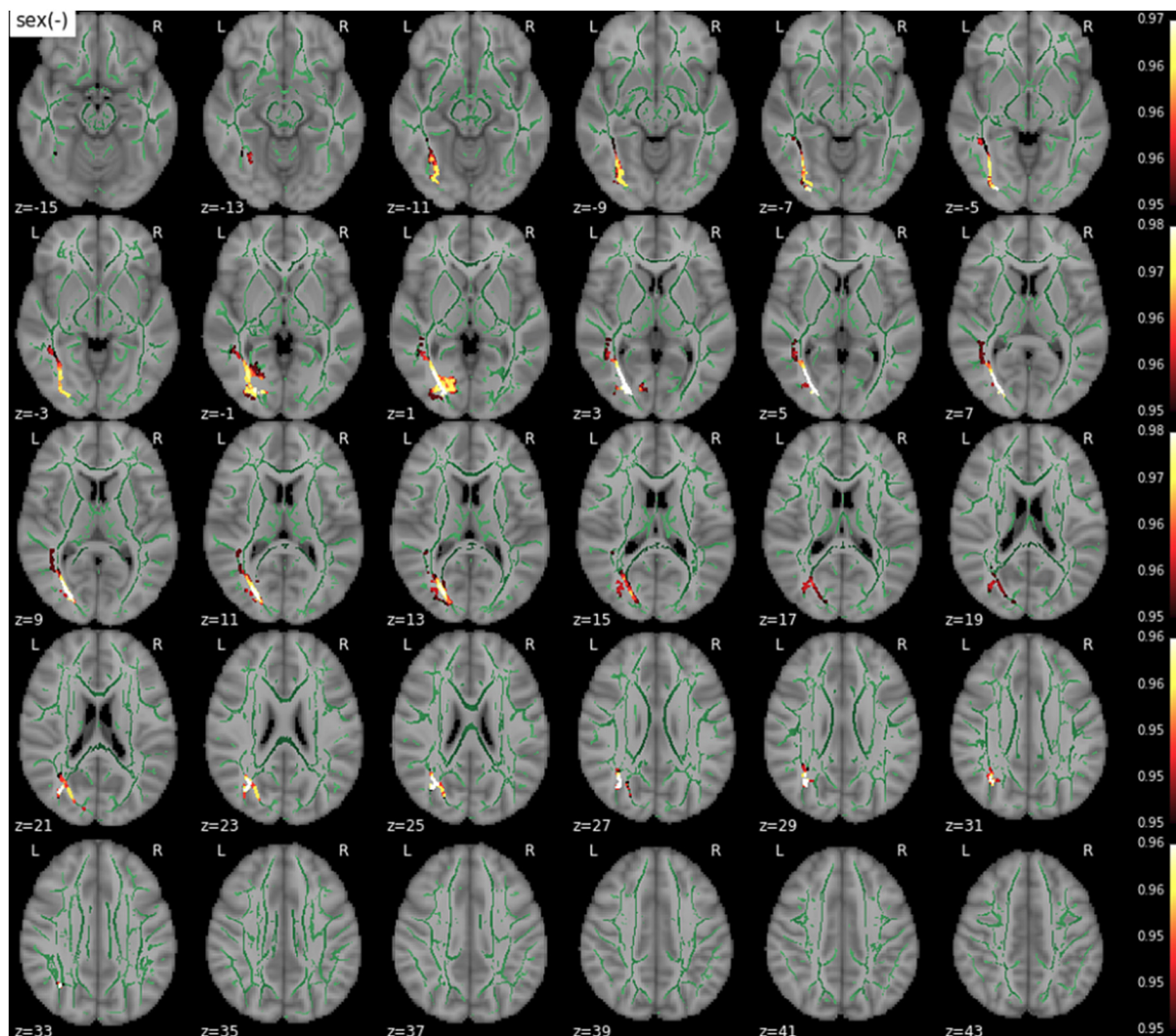
Fig. 6. Main effect of sex (females > males) on T1w/T2w ratios. The WM skeleton is shown in green. Supra-threshold clusters are presented in colors from dark red to white (1-p > .95, familywise error rate- and threshold-free cluster enhancement-corrected).

cognitively healthy participants preserves our dataset reasonably from these variations. We also fairly assume that the use of a permutation-based technique for group comparisons is particularly suited to the case of non-quantitative descriptors, which might fail the general statistical assumptions in standard parametric approaches.

Aside from this, to which particular signal issued from myelin content T1w/T2w ratios are sensitive is still being debated as well. Inconsistent correlations with histology, MT ratios (Arshad et al., 2017), multi-echo T2 (Uddin et al., 2018), or relaxometry (Hagiwara et al., 2018) suggest that T1w/T2w ratio may also be sensitive to additional microstructural properties such as axonal diameter (Arshad et al., 2017) or be driven by external influences, i.e. iron accumulation, calcium content, inflammation or atrophy (Uddin et al., 2018; Hagiwara et al., 2018). Nevertheless, while it is acknowledged that T1w/T2w ratio is not a specific index of myelin, it may still be recognized as a useful proxy in particular for group comparisons, such as in recent studies in multiple sclerosis (Nakamura et al., 2017; Righart et al., 2017). More research is needed both to better characterize the intimate nature of the T1w/T2w signal and more generally to address the true impact of demyelination in subjects at risk of developing AD.

In the AD continuum, structural markers are known to depart from their normal course long before cognitive decline typically begins. Additional pathological markers, such as cerebrospinal fluid ratios and brain amyloid burden, are thus required in order to screen preclinical

subjects among cognitively normal individuals. In this regard, this present study is currently limited by the absence of these markers. Cognitively healthy *APOE-ε4* homozygotes have been reported to show a significantly higher prevalence of cerebral amyloid pathology. At the mean age of our homozygote group (55 years), approximately 50% of these individuals display abnormal levels of amyloid biomarkers, as compared with only 10% of non-carriers and about 20% of carriers of a single *ε4* allele (Jansen et al., 2015). Besides, T1w/T2w ratio might show a positive association with Aβ accumulation (Bartzokis et al., 2007), according to recent results (Yasuno et al., 2017; Pelkmans et al., 2019). Still, such impact, as it was suggested, would come in a direction contrary to the one we find for the *APOE-ε4* status, therefore pinpointing the strength of the effect in our dataset regardless of the possible underlying amyloid charge. Eventually, access to follow-up information and complementary examination including positron emission tomographic imaging and lumbar puncture (Molinuevo et al., 2016) will allow us to mitigate this risk and to account for the influence of Aβ pathology and to better stratify our dataset with respect to preclinical AD research criteria.

The major strength of this study lies in having recruited a relatively young, cognitively healthy sample, with a very large number of *APOE-ε4* homozygotes. This allowed us to study individuals at three levels of risk, thus building on most published studies that compared carriers vs non-carriers. In complement to results obtained on DWI data on the

same participants, this present study adds to the emerging evidence that myelination may represent an important biomarker in the earliest stages of AD. This confirms the need for further investigation based on myelin imaging in order to specifically discriminate changes in myelination against other potential alterations in WM. This could resultantly pave the way for new promyelinating therapeutic strategies.

5. Conclusions

Our results show significantly decreased T1w/T2w ratio values in the WM of cognitively healthy carriers of the *APOE ε4* allele in a dose-dependent manner. Such variations in T1w/T2w ratio are consistent with differential changes previously observed in DWI metrics, giving further support to the interpretation of an alteration of the myelin sheath of axons at a stage preceding axonal loss. Further research involving specific myelin mapping sequences is required in order to decipher the observed discrepancies between T1w/T2w and DWI, and to achieve quantitative comparisons across *APOE-ε4* genotypic groups.

Acknowledgements

Appendix A. Supplementary data

Supplementary data to this article can be found online at https://doi.org/10.1016/j.nicl.2019.101983.

References

Adluru, N., Destiche, D.J., Lu, S.Y.F., Doran, S.T., Birdsill, A.C., Melah, K.E., Okonkwo, O.C., Alexander, A.L., Dowling, N.M., Johnson, S.C., Sager, M.A., Bendlin, B.B., 2014. White matter microstructure in late middle-age: effects of apolipoprotein E4 and parental family history of Alzheimer's disease. NeuroImage Clin. 4, 730–742.

Amlien, I.K., Fjell, A.A.M., 2014. Diffusion tensor imaging of white matter degeneration in Alzheimer's disease and mild cognitive impairment. Neuroscience 276, 206–215.

Arshad, M., Stanley, J.A., Raz, N., 2017. Test–retest reliability and concurrent validity of in vivo myelin content indices: myelin water fraction and calibrated T1w/T2w image ratio. Hum. Brain Mapp. 38, 1780–1790.

Avants, B.B., Tustison, N., Song, G., 2009. Advanced normalization tools (ANTS). Insight J 2, 1–35.

Bartzokis, G., 2004. Age-Related Myelin Breakdown: A Developmental Model of Cognitive Decline and Alzheimer's Disease. vol. 25. pp. 5–18.

Bartzokis, G., 2011. Alzheimer's disease as homeostatic responses to age-related myelin breakdown. Neurobiol. Aging 32, 1341–1371.

Bartzokis, G., Lu, P.H., Mintz, J., 2007. Human brain myelination and amyloid beta deposition in Alzheimer's disease. Alzheimer's Dementia 3, 122–125.

Benitez, A., Fieremans, E., Jensen, J.H., Falangola, M.F., Tabesh, A., Ferris, S.H., Helpern, J.A., 2014. White matter tract integrity metrics reflect the vulnerability of late-myelinating tracts in Alzheimer's disease. NeuroImage Clin. 4, 64–71.

Bouhrara, M., Reiter, D.A., Bergeron, C.M., Zukley, L.M., Ferrucci, L., Resnick, S.M., Spencer, R.G., 2018. Evidence of demyelination in mild cognitive impairment and dementia using a direct and specific magnetic resonance imaging measure of myelin content. Alzheimers Dement. 0, 1–7.

Brickman, A.M., Meier, I.B., Korgaonkar, M.S., Provenzano, F.A., Grieve, S.M., Siedlecki, K.L., Wasserman, B.T., Williams, L.M., Zimmerman, M.E., 2012. Testing the white matter retrogenesis hypothesis of cognitive aging. Neurobiol. Aging 33, 1699–1715.

Brugulat-Serrat, A., Rojas, S., Bargalló, N., Conesa, G., Minguillón, C., Fauria, K., … Gispert, J. D. (2017). Incidental findings on brain MRI of cognitively normal first-

degree descendants of patients with Alzheimer's disease: a cross-sectional analysis from the ALFA (Alzheimer and Families) project. BMJ Open, 7(3) (2017).

Buschke, H., 2014. Rationale of the memory binding test. In: Nilsson, Lars Göran, Ohta, N. (Eds.), Dementia and Memory. Psychology Press.

Cacciaglia, R., Molinuevo, J.L., Falcón, C., Brugulat-Serrat, A., SánchezBenavides, G., Gramunt, N., Esteller, M., Morán, S., Minguillón, C., Fauria, K., Gispert, J.D., 2018. Effects of APOE-e4 allele load on brain morphology in a cohort of middle-aged healthy individuals with enriched genetic risk for Alzheimer's disease. Alzheimers Dement. 14, 902–912.

Chen, K., Reiman, EM., Alexander, GE., Caselli, RJ., Gerkin, R., Bandy, D., Domb, A., Osborne, D., Fox, N., Crum, WR., Saunders, AM., Hardy, J., 2007. Correlations between apolipoprotein E epsilon4 gene dose and whole brain atrophy rates. Am J Psychiatry 164 (6), 916–921. Epub 2008 Apr 11. https://www.ncbi.nlm.nih.gov/pubmed/17541051.

Chen, H., Budin, F., Noel, J., Prieto, J.C., Gilmore, J., Rasmussen, J., Wadhwa, P.D., Entringer, S., Buss, C., Styner, M., 2017. White matter Fiber-based analysis of T1w/T2w ratio map. Proc. SPIE. Int. Soc. Optical Engg. 10133.

Dean, D.D.C., Jerskey, B.B.A., Chen, K., Protas, H., Thiyyagura, P., Roontiva, A., O'Muircheartaigh, J., Dirks, H., Waskiewicz, N., Lehman, K., Siniard, A.L., Turk, M.N., Hua, X., Madsen, S.K., Thompson, P.M., Fleisher, A.S., Huentelman, M.J., Deoni, S.C.L., Reiman, E.M., Reiman, E.M., 2014. Brain differences in infants at differential genetic risk for late- onset Alzheimer disease: a Cross-sectional imaging study. JAMA Neurol. 71, 11–22.

Dean, D.C., Sojkova, J., Hurley, S., O'Grady, P., Canda, C.-M., Davenport, N.J., Asthana, S., Sager, M.A., Johnson, S.C., Alexander, A.L., Bendlin, B.B., 2015. ApoE-e4 is associated with altered myelin content in preclinical ad. Alzheimers Dement. 11, P425.

Dean, D.C., Hurley, S.A., Kecskemeti, S.R., O'Grady, J.P., Canda, C., Davenport-Sis, N.J., Carlsson, C.M., Zetterberg, H., Blennow, K., Asthana, S., Sager, M.A., Johnson, S.C., Alexander, A.L., Bendlin, B.B., 2017. Association of amyloid pathology with myelin alteration in preclinical Alzheimer disease. JAMA Neurol. 74, 41–49.

Deoni, S.C., Rutt, B.K., Arun, T., Pierpaoli, C., Jones, D.K., 2008. Gleaning multi-component T1 and T2 information from steady-state imaging data. Magn. Reson. Med. 60, 1372–1387.

Douaud, G., Jbabdi, S., Behrens, T.E.J., Menke, R.A., Gass, A., Monsch, A.U., Rao, A., Whitcher, B., Kindlmann, G., Matthews, P.M., Smith, S., 2011. DTI measures in crossing-fibre areas: increased diffusion anisotropy reveals early white matter alteration in MCI and mild Alzheimer's disease. NeuroImage 55, 880–890.

Fouquet, M., Besson, F.L., Gonneaud, J., La Joie, R., Chételat, G., 2014. Imaging brain effects of APOE4 in cognitively Normal individuals across the lifespan. Neuropsychol. Rev. 24, 290–299.

Ganzetti, M., Wenderoth, N., Mantini, D., 2014. Whole brain myelin mapping using T1- and T2-weighted MR imaging data. Front. Hum. Neurosci. 8 (671).

Gao, J., Cheung, R.T.F., Lee, T.M., Chu, L.W., Chan, Y.S., Mak, H.K.F., Zhang, J.X., Qiu, D., Fung, G., Cheung, C., 2011. Possible retrogenesis observed with fiber tracking: an anteroposterior pattern of white matter disintegrity in normal aging and alzheimer's disease. J. Alzheimers Dis. 26, 47–58.

Glasser, M.F., Van Essen, D.C., 2011. Mapping human cortical areas in vivo based on myelin content as revealed by T1- and T2-weighted MRI. J. Neurosci. 31, 11597–11616.

Glasser, M.F., Goyal, M.S., Preuss, T.M., Raichle, M.E., Van Essen, D.C., 2014. Trends and properties of human cerebral cortex: correlations with cortical myelin content. Neuroimage 93, 165–175.

Gramunt, N., Buschke, H., Sánchez-Benavides, G., Lipton, R.B., Peña-Casanova, J., Diéguez-Vide, F., Masramon, X., Gispert, J.D., Fauria, K., Camí, J., Molinuevo, J.L., Garre-Olmo, J., 2015. Reference data of the Spanish memory binding test in a midlife population from the ALFA STUDY (Alzheimer's and family). J. Alzheimers Dis. 48, 613–625.

Grydeland, H., Vertes, P.E., Váša, F., Romero-Garcia, R., Whitaker, K., Alexander-Bloch, A.F., Bjørnerud, A., Patel, A.X., Sederevičius, D., Tamnes, C.K., Westlye, L.T., 2018. Waves of maturation and senescence in micro-structural MRI markers of human cortical myelination over the lifespan. Cereb. Cortex 29 (3), 1369–1381.

Hagiwara, A., Hori, M., Kamagata, K., Warntjes, M., Matsuyoshi, D., Nakazawa, M., Ueda, R., Andica, C., Koshino, S., Maekawa, T., Irie, R., Takamura, T., Kumamaru, K.K., Abe, O., Aoki, S., 2018. Myelin measurement: comparison between simultaneous tissue Relaxometry, magnetization transfer saturation index, and T1w/T2w ratio methods. Sci. Rep. 8, 10554.

Heath, F., Hurley, S.A., Johansen-Berg, H., Sampaio-Baptista, C., 2018. Advances in Noninvasive Myelin Imaging. vol. 78. pp. 136–151.

Iwatani, J., Ishida, T., Donishi, T., Ukai, S., Shinosaki, K., Terada, M., Kaneoke, Y., 2015. Use of T1-weighted/T2-weighted magnetic resonance ratio images to elucidate changes in the schizophrenic brain. Brain Behav. 5 n/a-n/a.

Jansen, W.J., Ossenkoppele, R., Knol, D.L., Tijms, B.M., Scheltens, P., Verhey, F.R.J., Visser, P.J., Aalten, P., … Zetterberg, M., 2015. H. Prevalence of cerebral amyloid pathology in persons without dementia. JAMA 313, 1924.

Jenkinson, M., Beckmann, C.F., Behrens, T.E., Woolrich, M.W., Smith, S.M., 2012. FSL. vol. 62. pp. 782–790.

Lebel, C., Deoni, S., 2018. The Development of Brain White Matter Microstructure.

Lemaître, H., Crivello, F., Dufouil, C., Grassiot, B., Tzourio, C., Alpérovitch, A., Mazoyer, B., 2005. No epsilon4 gene dose effect on hippocampal atrophy in a large MRI database of healthy elderly subjects. Neuroimage 24 (4), 1205–1213. Epub 2004 Dec 10. https://www.ncbi.nlm.nih.gov/pubmed/15670698.

Lee, K., Cherel, M., Budin, F., Gilmore, J., Zaldarriaga Consing, K., Rasmussen, J., Wadhwa, P.D., Entringer, S., Gilmore, J., Glasser, M.F., Van Essen, D.C., Buss, C., Styner, M., 2015. Early postnatal myelin content estimate of white matter via T1w/T2w ratio. 9417, 94171R.

Liu, C.-C., Liu, C.-C., Kanekiyo, T., Xu, H., 2013a. Bu, G. apolipoprotein E and Alzheimer

disease: risk, mechanisms and therapy. Nat. Rev. Neurol. 9 (2), 106–118.

Liu, J., Yin, C., Xia, S., Jia, L., Guo, Y., Zhao, Z., Li, X., Han, Y., Jia, J., 2013b. White matter changes in patients with amnestic mild cognitive impairment detected by diffusion tensor imaging. PLoS ONE 8, e59440.

Lu, P.H., Lee, G.J., Tishler, T.A., Meghpara, M., Thompson, P.M., Bartzokis, G., 2013. Myelin breakdown mediates age-related slowing in cognitive processing speed in healthy elderly men. Brain Cogn. 81, 131–138.

Manjón, J.V., Coupé, P., Concha, L., Buades, A., Collins, D.L., Robles, M., 2013. Diffusion weighted image Denoising using Overcomplete local PCA. PLoS ONE 8, e73021.

Molinuevo, J.L., Gramunt, N., Gispert, J.D., Fauria, K., Esteller, M., Minguillon, C., Sánchez-Benavides, G., Huesa, G., Morán, S., Dal-Ré, R., Camí, J., 2016. The ALFA project: a research platform to identify early pathophysiological features of Alzheimer's disease. Alzheimer's Dementia (New York, N. Y.) 2, 82–92.

Nakamura, K., Chen, J.T., Ontaneda, D., Fox, R.J., Trapp, B.D., 2017. T1 − /T2 weighted ratio differs in demyelinated cortex in multiple sclerosis. Ann. Neurol. 82, 635–639.

Nasrabady, S.E., Rizvi, B., Goldman, J.E., Brickman, A.M., 2018. White matter changes in Alzheimer's disease: a focus on myelin and oligodendrocytes. Acta Neuropathol. Commun. 6 (22).

Operto, G., Cacciaglia, R., Grau-Rivera, O., Falcon, C., Brugulat-Serrat, A., Ródenas, P., Ramos, R., Morán, S., Esteller, M., Bargalló, N., Molinuevo, J., Gispert, J., 2018. White matter microstructure is altered in cognitively normal middle-aged APOE-4 homozygotes. Alzheimers Res. Ther. 10.

Pelkmans, W., Dicks, E., Barkhof, F., Vrenken, H., Scheltens, P., van der Flier, W.M., Tijms, B.M., 2019. Gray matter T1-w/T2-w ratios are higher in Alzheimer's disease. Hum. Brain Mapp. 40 (13), 3900–3909. https://www.ncbi.nlm.nih.gov/pubmed/31157938 (Epub 2019 Jun 3).

Peters, A., 2002. The Effects of Normal Aging on Myelin and Nerve Fibers: A Review. vol. 31. pp. 581–593.

Pievani, M., Agosta, F., Pagani, E., Canu, E., Sala, S., Absinta, M., Geroldi, C., Ganzola, R., Frisoni, G.B., Filippi, M., 2010. Assessment of white matter tract damage in mild cognitive impairment and Alzheimer's disease. Hum. Brain Mapp. 31, 1862–1875.

Protas, HD., Chen, K., Langbaum, JB., Fleisher, AS., Alexander, GE., Lee, W., Bandy, D., de Leon, MJ., Mosconi, L., Buckley, S., Truran-Sacrey, D., Schuff, N., Weiner, MW., Caselli, RJ., Reiman, EM., 2013. Posterior cingulate glucose metabolism, hippocampal glucose metabolism, and hippocampal volume in cognitively normal, late-middle-aged persons at 3 levels of genetic risk for Alzheimer disease. JAMA Neurol. 70 (3), 320–325. Epub 2004 Dec 10. https://www.ncbi.nlm.nih.gov/pubmed/23599929.

Reiman, E.M., Caselli, R.J., Chen, K., Alexander, G.E., Bandy, D., Frost, J., 2001. Declining brain activity in cognitively normal apolipoprotein E epsilon 4 heterozygotes: a foundation for using positron emission tomography to efficiently test treatments to prevent Alzheimer's disease. Proc. Natl. Acad. Sci. U. S. A. 98, 3334–3339.

Reiman, E.M., Chen, K., Liu, X., Bandy, D., Yu, M., Lee, W., Ayutyanont, N., Keppler, J., Reeder, S.A., Langbaum, J.B.S., Alexander, G.E., Klunk, W.E., Mathis, C.A., Price, J.C., Aizenstein, H.J., DeKosky, S.T., Caselli, R.J., 2009. Fibrillar amyloid-beta burden in cognitively normal people at 3 levels of genetic risk for Alzheimer's disease. Proc. Natl. Acad. Sci. U. S. A. 106, 6820–6825.

Reinvang, I., Espeseth, T., Westlye, L.T., 2013. APOE-Related Biomarker Profiles in Non-pathological Aging and Early Phases of Alzheimer's Disease. vol. 37. pp. 1322–1335.

Reisberg, B., Franssen, EH., Souren, LE., Auer, SR., Akram, I., Kenowsky, S., 2009. Evidence and mechanisms of retrogenesis in Alzheimer's and other dementias: management and treatment import. Am. J. Alzheimers Dis. Other Demen 17 (4), 202–212. Epub 2008 Apr 11. https://www.ncbi.nlm.nih.gov/pubmed/12184509.

Righart, R., Biberacher, V., Jonkman, L.E., Klaver, R., Schmidt, P., Buck, D., Berthele, A., Kirschke, J.S., Zimmer, C., Hemmer, B., Geurts, J.J.G., Mühlau, M., 2017. Cortical pathology in multiple sclerosis detected by the T1/T2 weighted ratio from routine magnetic resonance imaging. Ann. Neurol. 82, 519–529.

Shafee, R., Buckner, R.L., Fischl, B., 2015. Gray matter myelination of 1555 human brains using partial volume corrected MRI images. NeuroImage 105, 473–485.

Jonathan E., Sherin, George, Bartzokis., 2011. Chapter 15 - Human Brain Myelination Trajectories Across the Life Span: Implications for CNS Function and Dysfunction. In: Austad, Steven N., Masoro, Edward J. (Eds.), Handbooks of Aging, Handbook of the Biology of Aging. 34. Academic Press, pp. 333–346. https://doi.org/10.1016/B978-0-12-378638-8. ISBN: 9780123786388. https://www.sciencedirect.com/science/article/pii/B9780123786388000154.

Smith, S.M., Jenkinson, M., Johansen-Berg, H., Rueckert, D., Nichols, T.E., Mackay, C.E., Watkins, K.E., Ciccarelli, O., Cader, M.Z., Matthews, P.M., Behrens, T.E., 2006. Tract-based spatial statistics: Voxelwise analysis of multi-subject diffusion data. NeuroImage 31, 1487–1505.

Smith, S., Nichols, TE., 2009. Threshold-free cluster enhancement: addressing problems of smoothing, threshold dependence and localisation in cluster inference. Neuroimage 44 (1), 333–346. https://doi.org/10.1109/TMI.2015.2419072. Epub 2008 Apr 11. https://www.ncbi.nlm.nih.gov/pubmed/18501637.

Song, S.K., Sun, S.W., Ramsbottom, M.J., Chang, C., Russell, J., Cross, A.H., 2002. Dysmyelination revealed through MRI as increased radial (but unchanged axial) diffusion of water. NeuroImage 17, 1429–1436.

Soun, J.E., Liu, M.Z., Cauley, K.A., Grinband, J., 2017. Evaluation of neonatal brain myelination using the T1- and T2-weighted MRI ratio. J. Magn. Reson. Imaging 46, 690–696.

Sudre, CH., Cardoso, MJ., Bouvy, WH., Biessels, GJ., Barnes J, Ourselin S., 2015. Bayesian model selection for pathological neuroimaging data applied to white matter lesion segmentation. IEEE Trans. Med. Imaging 34 (10), 2079–2102. https://doi.org/10.1109/TMI.2015.2419072. Epub 2015 Apr 2. https://www.ncbi.nlm.nih.gov/pubmed/25850086.

Stricker, N.H., Schweinsburg, B.C., Delano-Wood, L., Wierenga, C.E., Bangen, K.J., Haaland, K.Y., Frank, L.R., Salmon, D.P., Bondi, M.W., 2009. Decreased white matter integrity in late-myelinating fiber pathways in Alzheimer's disease supports retro-genesis. NeuroImage 45, 10–16.

Uddin, M.N., Figley, T.D., Marrie, R.A., Figley, C.R., 2018. Can T1w/T2w ratio be used as a myelin-specific measure in subcortical structures? Comparisons between FSE-based T1w/T2w ratios, GRASE-based T1w/T2w ratios and multi-echo GRASE-based myelin water fractions. NMR Biomed. 31, e3868.

Wakana, S., Jiang, H., Nagae-Poetscher, L.M., van Zijl, P.C.M., Mori, S., 2004. Fiber tract–based atlas of human white matter anatomy. Radiology 230 (1), 77–87.

Wang, Y., Sun, P., Wang, Q., Trinkaus, K., Schmidt, R.E., Naismith, R.T., Cross, A.H., Song, S.K., 2015. Differentiation and quantification of inflammation, demyelination and axon injury or loss in multiple sclerosis. Brain 138, 1223–1238.

Welker, K.M., Patton, A., 2012. Assessment of normal myelination with magnetic resonance imaging. Semin. Neurol. 32 (15–28).

Winkler, A.M., Ridgway, G.R., Webster, M.A., Smith, S.M., Nichols, T.E., 2014. Permutation inference for the general linear model. NeuroImage 92, 381–397.

Yasuno, F., Kazui, H., Morita, N., Kajimoto, K., Ihara, M., Taguchi, A., Yamamoto, A., Matsuoka, K., Takahashi, M., Nakagawara, J., Iida, H., Kishimoto, T., Nagatsuka, K., 2017. Use of T1-weighted/T2-weighted magnetic resonance ratio to elucidate changes due to amyloid β accumulation in cognitively normal subjects. NeuroImage Clin. 13, 209–214.

Yeatman, J.D., Dougherty, R.F., Myall, N.J., Wandell, B.A., Feldman, H.M., 2012. Tract profiles of white matter properties: automating Fiber-tract quantification. PLoS ONE 7, e49790.

Zhang, J., Aggarwal, M., Mori, S., 2012. Structural insights into the rodent CNS via diffusion tensor imaging. Trends Neurosci. 35, 412–421.